ACS APPLIED MATERIALS & INTERFACES

RESEARCH ARTICLE

www.acsami.org

8-Aminoquinoline Functionalized Silica Nanoparticles: A Fluorescent Nanosensor for Detection of Divalent Zinc in Aqueous and in Yeast Cell Suspension

Shiva K. Rastogi,[*,†,‡] Parul Pal,[†,‡] D. Eric Aston,[§] Thomas E. Bitterwolf,[†] and A. Larry Branen[⊥]

[†]Department of Chemistry, University of Idaho, Moscow, Idaho 83844-2343, United States

[§]Department of Chemical and Materials Engineering, University of Idaho, Moscow, Idaho 83844-1021, United States

[⊥]Biosensors and Nanotechnology Applications Laboratory, University of Idaho, Coeur d'Alene, Idaho 83814-2277, United States

Supporting Information

ABSTRACT: Zinc is one of the most important transition metal of physiological importance, existing primarily as a divalent cation. A number of sensors have been developed for Zn(II) detection. Here, we present a novel fluorescent nanosensor for Zn(II) detection using a derivative of 8-aminoquinoline (N-(quinolin-8-yl)-2-(3 (triethoxysilyl)propylamino)acetamide (QTEPA) grafted on silica nanoparticles (SiNPs). These functionalized SiNPs were used to demonstrate specific detection of Zn(II) in tris-HCl buffer (pH 7.22), in yeast cell (*Saccharomyces cerevisiae*) suspension, and in tap water. The silane QTEPA, SiNPs and final product were characterized using solution and solid state nuclear magnetic resonance, Fourier transform infrared, ultraviolet−visible absorption spectroscopy, transmission electron microscopy, elemental analysis, thermogravimetric techniques, and fluorescence spectroscopy. The nanosensor shows almost 2.8-fold fluorescence emission enhancement and about 55 nm red-shift upon excitation with 330 ± 5 nm wavelength in presence of 1 μM Zn(II) ions in tris-HCl (pH 7.22). The presence of other metal ions has no observable effect on the sensitivity and selectivity of nanosensor. This sensor selectively detects Zn(II) ions with submicromolar detection to a limit of 0.1 μM. The sensor shows good applicability in the determination of Zn(II) in tris-HCl buffer and yeast cell environment. Further, it shows enhancement in fluorescence intensity in tap water samples.

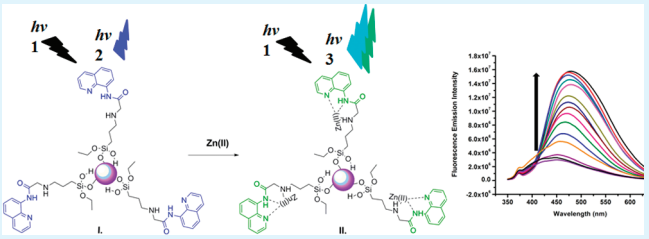

KEYWORDS: silica nanoparticles, 8-aminoquinoline, Zn(II) sensor, tris-HCl buffer, yeast cells, fluorescence detection

1. INTRODUCTION

In the past decade, there has been a growing interest in the development of optical molecular chemosensors using nanomaterials for cations and anions.[1−8] However, there is still a lack of highly selective and sensitive molecular chromo or fluorogenic sensors for a number of target species. Early investigations for sensing metal ions were carried out on the neuromodulatory roles of common biological metal ion K(I)[9] and Ca(II).[10] The d-block metal ions, such as Mn(II),[11] Fe(II),[12] Cu(II),[13] and Zn(II),[14] also play an important role in neurobiology, metabolism, and catalysis.[15] Among them, designing and fabricating fluorescent nanomaterials for the detection of zinc cation has drawn more attention.[16] Zn(II) is one of the most important transition metal ions found in the human body, and it plays multiple roles in both extra- and intracellular functions, such as in gene transcription[17] and metalloenzymes.[18] In addition to having a beneficial role in the human body, it is closely related to severe pathological diseases, such as Alzheimer's and Parkinson's diseases,[19] in synaptic neurotransmission,[20] and in mediating neuronal exotoxicity.[21]

Many optical chemosensors have been developed on the basis of organic fluorophores and organofunctionalized nanomaterials in the past few years,[22−25] which can selectively detect Zn(II) in solution. However, the advantage of functionalized nanomaterials over "naked" sensors is the reduction of interference by protein binding or membrane binding of the latter.[26,27] Additionally, the organic−inorganic framework of nanomaterial may provide protection of the sensor probe. Therefore, functionalized nanomaterial sensors would also be a useful and a needed tool for metal ion detection in extra- and intracellular environment.

Most of the Zn(II) sensors reported over the years have been developed from quinoline derivatives, such as 6-methoxy-(8-p-tolunesulphonamido) quinoline (TSQ),[28] Zinquin[29−31] and TFLZn (TSQ analogue).[32] These aryl sulfonamides of quinolines incorporate macro cyclic Zn(II) binding units, and were used for fluorescence imaging upon Zn(II) binding. Nonetheless, the supramolecular system of quinolines, especially 8-aminoquinoline, offer an attractive option for developing highly selective Zn(II) sensors even over other possible competing cations.[33] The simplest example of the use of 8-aminoquinoline derivative

Received: February 24, 2011
Accepted: April 21, 2011
Published: April 21, 2011

Scheme 1. (i) Absolute EtOH (0.8 mmol); [DIW]/[TEOS]; Sonicated for 2 h at 45 °C and 28-30% aq NH_3 (1.87 mmol) Solution Was Added Dropwise (0.03 mL/min) and Sonicated for 8 h at 45 ± 5 °C. (ii) 8-Aminoquinoline (8 mmol); Chloroacetyl Chloride (9.6 mmol); Pyridine (11.2 mmol); CH_2Cl_2 (50 mL); 0 °C to rt, 2 h. (iii) 3-Aminopropyltriethoxysilane (2.5 mmol); Anhyd. K_2CO_3 (3.41 mmol) and 4 (2.27 mmol), Dry CH_3CN (40 mL) rt to Δ for 4 h. (iv) SiNPs (100 mg); Anhyd. Toluene (40 mL); 0.015 mmol of 5, Δ for 8 h; Addition of Zn(II) Ions in the Suspension of 6 Results in Enhancement of Fluorescence Intensities II

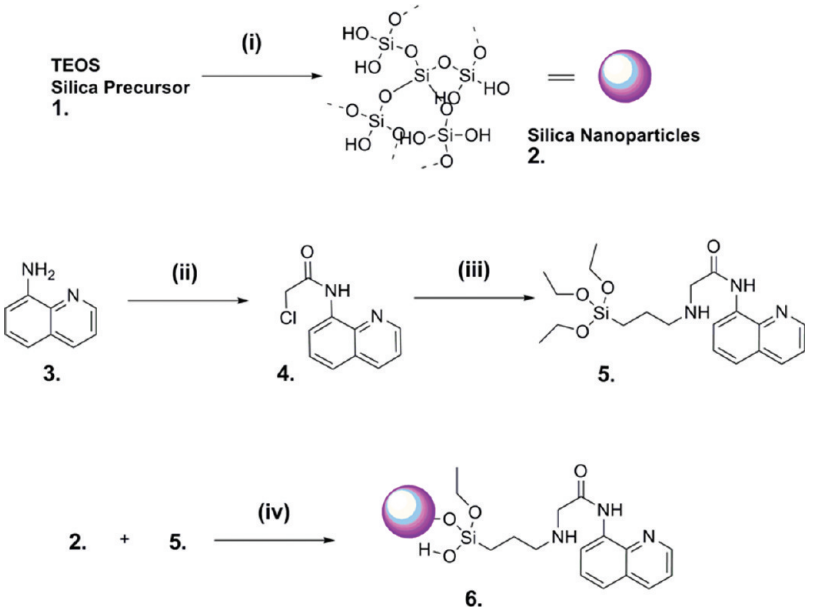

for Zn(II) detection was recently described by Zhang et al.[34] and Dong et al.[35]

The operation of these sensors is mostly based on signal amplification as a result of binding Zn(II). This phenomenon, also termed chelation enhanced fluorescence (CHEF), operates on the mechanism of photoinduced electron transfer (PET).[26,36−39] In the case of 8-aminoquinoline, the lone pair of electrons of the 8-amino residue is transferred to the π-system of the fluorophore upon excitation, which, in turn, results in suppressing the fluorescence intensity. The involvement of the lone pair of electrons in binding the metal ions inhibits the PET process, resulting in the increase of fluorescence intensities. This phenomenon is preferred as it is visually perceptive. This principle is applied in most of the Zn(II) sensors, a process that is well-studied and explained in several reviews.[40−43]

In this study, we selected a chloroacetyl derivative of 8-aminoquinoline as the fluorophore, supported on silica nanoparticles (SiNPs) as sophisticated hosts, for binding Zn(II). However, we have recently reported the use of ordered mesoporous silica MCM-41 functionalized with the same fluorophore, N-(quinolin-8-yl)-2-(3-(triethoxysilyl)propylamino)acetamide (QTEPA), for fluorescent detection of Zn(II)[44] (Scheme 1). But, the current study is an extension of the previous one in order to explore the effect of difference in morphology between MCM-41 and SINPs on the overall performance of the sensor. The SiNPs provide their outer surface for modification as against the limited functionalization (depending on the size of the organic moiety) of inner channels in MCM-41. Further, silica nanoparticles are particularly attractive as they are easy to synthesize, are aqueous solution friendly, and can be easily engineered to various sizes and shapes.[45] These QTEPA functionalized SiNPs, to the best of our knowledge, are the first to be reported for the selective and sensitive fluorogenic detection of Zn(II) in tris-HCl buffer solution, and in yeast (*Saccharomyces cerevisiae*) cells.

2. EXPERIMENTAL SECTION

2.1. Materials. All the chemicals and reagents were purchased from Sigma Aldrich, St. Louis, MO, USA, and Fisher Scientific, New Jersey, and used without further purification. The solvents used for reactions were stored in brown bottles with appropriate drying agents, and freshly distilled before use. NaCl, KCl, $CaCl_2$, $MgCl_2$, $MnCl_2$, $FeCl_2$, $FeCl_3$, $CoCl_2$, $NiCl_2$, $CuSO_4 \cdot 5H_2O$, $CdCl_2$, $HgCl_2$, $PbNO_3$, $TlNO_3$, $ZnNO_3 \cdot 6H_2O$, $ZnSO_4 \cdot 7H_2O$, $Zn(CH_3CO)_2 \cdot 2H_2O$, $Zn(CN)_2$, $Zn(ClO_4)_2 \cdot 6H_2O$, $ZnCl_2$, $ZnBr_2$, and ZnI_2 were of analytical grade. Doubly distilled deionized water (DIW) was used for all experiments, and the solution NMR was carried out in DMSO-d_6, Tetraethylorthosilicate (TEOS) 99.9% and absolute ethanol (99.5%) were purchased from Sigma-Aldrich. All the glassware was cleaned using aqua-regia for 16 h at rt, rinsed several times with DIW followed by treatment with 10% HF/DIW solution overnight at rt and rinsed several times with DIW and EtOH.

2.2. Instruments. ^{1}H NMR and ^{13}C NMR on solution samples, and ^{29}Si NMR and ^{13}C NMR on solid samples were measured on a Bruker Avance 500 MHz spectrometer. All of the solid state NMR spectra were measured using a 4 mm (o.d.) zirconia rotor with Kel-F cap. Solid state ^{29}Si NMR was performed under magic-angle spinning (MAS) conditions with a pulse delay of 1 min and a spinning rate of 12 kHz. For solid ^{13}C NMR, cross-polarization (CP) along with MAS was used with pulse delay of 2 s and spinning rate of 7−8 Hz. Chemical shifts for MAS ^{29}Si NMR were referenced to the external standard TMS. All solid and solution NMR experiments were performed at room temperature.

The functionalized SiNPs were characterized using Nicolet AVATAR 370DTGS FTIR model (Thermo Electron Corporation) and spectra were analyzed using OMNIC 7.4.127; UI Smart Performer software.

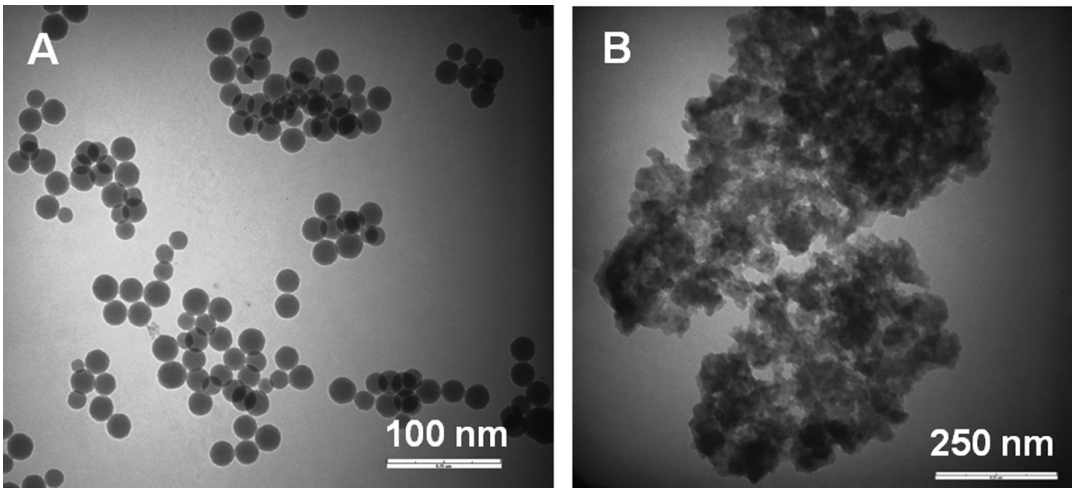

Figure 1. TEM images of (A) unmodified SiNPs and (B) modified SiNPs **6**, where the scale bar =100 and 250 nm, respectively.

Ultrasonic cleaner (FS30H; 42 kHz ± 6%) from Fisher Scientific was used for synthesis of silica NPs. TEM images were obtained on a JEOL 1200 EX II TEM equipped with LaB6 gun with 0.5 nm resolution. Thermogravimetric analysis (TGA) was carried out on a TGA Q50 V6.7 instrument. All TGA experiments were carried out under nitrogen atmosphere at a heating rate of 10 °C/min from 22 to 800 °C. An Exeter CE440 elemental analyzer was used to determine the C, H, and N content. Fluorescence and absorption spectra were acquired with a FluoroMax-3 spectrometer (Jobin Yvon Horiba) and a Shimadzu UV−vis spectrophotometer, respectively.

2.3. Synthesis of 6. The synthesis and characterization of **2** to **6** have been well-explained in the Supporting Information

2.4. Fluorescence Studies for Metal Ion Detection. Each detection of metal ion was measured in 0.01 M tris-HCl buffer at pH 7.22. The stock solution of modified SiNPs **6** was prepared in DIW (10.0 mg/2.0 mL). The concentration of **6** in the test solutions for fluorescence measurements was kept at a constant value of 100.0 μg/2.0 mL. Stock solutions of 0.1 M concentration of $ZnNO_3 \cdot H_2O$, NaCl, KCl, $CaCl_2$, $MgCl_2$, $MnCl_2$, $FeCl_2$, $FeCl_3$, $CuSO_4.5H_2O$, $CoCl_2$, $NiCl_2$, $CdCl_2$, $HgCl_2$, $PbNO_3$, and $TlNO_3$ were prepared in DIW. Necessary dilutions were made according to each experimental set up. All fluorescence spectra were recorded at 22 °C with the excitation wavelength of 330 ± 5 nm.

2.5. Yeast Strain/Growth Condition and Florescence Measurement. Yeast (*S. cerevisiae; Baker Yeast*)[34] was obtained from local retailer and used as a cell model. Before use, it was dispersed in YPD medium (1% yeast extract, 4.0% peptones, 2.0% glucose, 0.2% $(NH_4)_2SO_4$) and incubated for 12 h at 37 °C. The incubated yeast cells were mixed with SiNPs **6** at a final concentration of 100 μg/2 mL and incubated further for 1 h at 37 °C. The same experiment was performed with preheated (100 °C for 10 min) yeast cell suspension. The fluorescence emission measurement was carried out as described in above section.

3. RESULTS AND DISCUSSION

3.1. Synthesis and Characterization of 6. The study described here is based on design and development of a fluorescence optical sensor containing SiNPs functionalized with a metal ion chelating group. The surface of silica nanoparticles was modified by the organosilane QTEPA **5**, as shown in Scheme 1. The structural information of the fluorophore on the surface of silica nanoparticles was studied by solid-state characterization techniques: TEM imaging, TGA, elemental analysis, FT-IR, and NMR.

The TEM image of the SiNPs used in this study is shown in Figure 1A. The shape of these SiNPs was close to spherical with an average particle diameter of about 40 ± 10 nm. But, after treating the SiNPs with the silane **5**, the two undergo copolymerization, giving the final composite in the range of 200−300 nm size particles, which comprises a network of irregular shaped SiNPs as shown in Figure 1B.

The TGA weight loss curves for modified and unmodified SiNPs (Figure 2) provide a qualitative comparison of the changes induced after modification. The unmodified SiNPs (Figure 2A) exhibit a weight loss at about 71 °C corresponding to the loss of physically adsorbed water, suggesting the surface to be hydrophilic in nature.[46,47] With increase in temperature the weight loss remains constant, indicating no appreciable condensation of silanol groups on the surface. There is a significant change in the weight loss curve with modification of SiNPs (Figure 2B). The resulting pattern in the weight loss curve depends on the nature of the ligand, and the step transition shows the decomposition of the bonded organosilane with the height being roughly proportional to the carbon content.[48] In Figure 2B, a major weight loss region is seen between 265 and 546 °C, indicative of decomposition of the organic ligand chemically bonded to the surface. Further, the presence of the organic moiety on the surface was quantified using elemental analysis. The result gives the C/N molar ratio as 4.73 (Table 1 in the Supporting Information), which is almost the same as that of the organosilane **5** having released the three ethoxy groups, C/N = 4.66.[49] This is an indication that the functional group is grafted on the surface and did not decompose during the modification process.

The FT-IR spectra of modified and unmodified SiNPs are shown in Figure 3. In Figure 3A, the broad band centered at 3458.5 cm^{-1} represents the surface silanols, and any adsorbed moisture on the surface of unmodified SiNPs. The band at 1642.7 cm^{-1} represents the bending mode of O−H vibrations. The intense band centered at 1081.7 cm^{-1} is assigned to structural Si−O−Si vibrations, whereas the Si−OH vibration band is shown in the region 790−970 cm^{-1}. Compared to modified SiNPs **6** (Figure 3B), the silanol band disappears, whereas the N−H vibration band appears at 3273 cm^{-1}. The

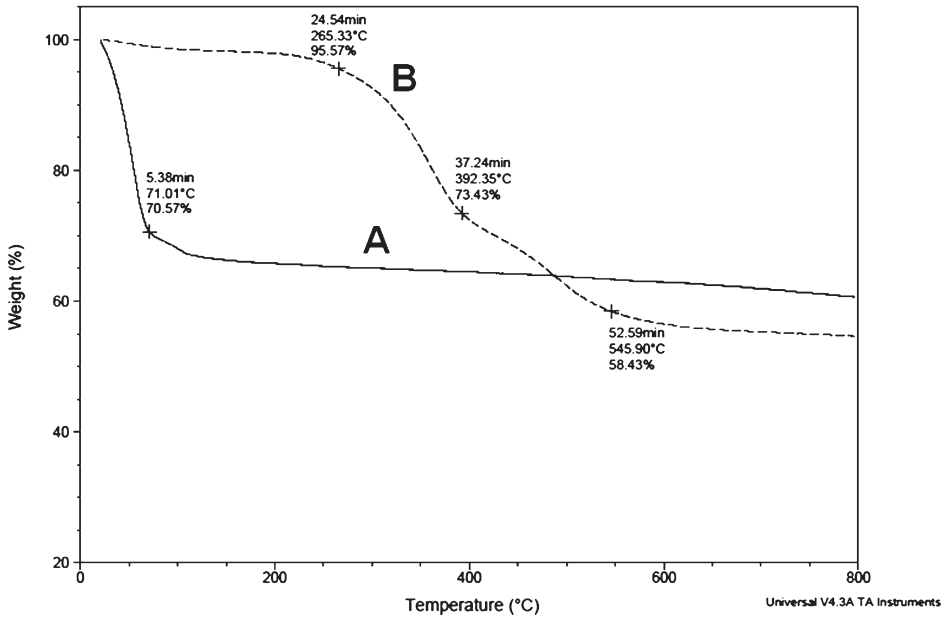

Figure 2. TGA weight-loss curves of (A) unmodified SiNPs (solid line) and (B) modified SiNPs **6** (dashed line).

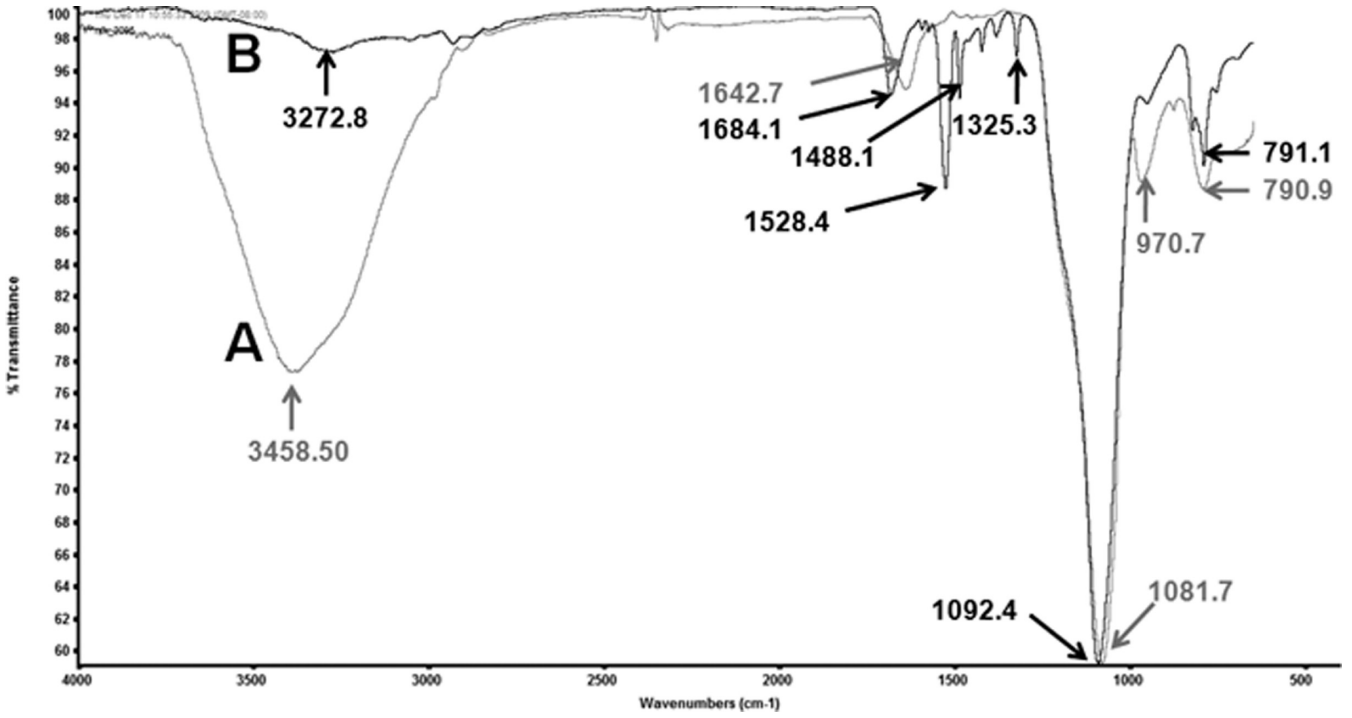

Figure 3. FTIR spectra of (A) unmodified SiNPs (gray line) and (B) modified SiNPs **6** (black line).

band at 1528.4 cm^{-1} is attributed to the C═C aromatic stretch, while the carbonyl band is observed at 1684.4 cm^{-1}. The region 1325−1488 cm^{-1} corresponds to aliphatic C−H stretching bands. The FT-IR spectra clearly indicate the presence of the silane **5** on the surface of SiNPs. Further, the presence of silane as part of the SiNPs is confirmed by solid-state ^{13}C and ^{29}Si NMR, shown in Figures SI4 and SI5, respectively, in the Supporting Information.

Comparative UV−vis absorption spectra are shown in Figure SI10 in the Supporting Information. The absorption maxima of 8-aminoquinoline **3** appears at 330 nm, whereas those of the chloroacetyl derivative **4** and the silane **5** show almost the same absorption maxima in the region around 315 nm. The UV−vis absorption spectrum of **6** shows similar maximum from 320 to 340 nm, indicating that grafting of **5** on SiNPs does not affect the inherent property of the 8-aminoquinoline fluorophore. The UV−vis spectrum of unmodified SiNPs does not show any band in the fluorophore region and serves as a negative control. The excitation wavelength of **6** and **6**+Zn(II) samples in tris-HCl buffer were also measured as shown in Figure SI11 in the

Supporting Information. The excitation and UV−vis absorption spectra correspond with each other and shows a broad band between 300 and 345 nm with the max at 330 nm. On the basis of these results, we selected the excitation wavelength of 330 ± 5 nm for all the fluorescence experiments.

3.2. pH Effect on Sensor. The performance characteristic of the sensor system was monitored for its sensitivity toward different pH conditions. It is essential for the sensor to perform satisfactorily at physiological pH for its application toward biological sensing. The response of the sensor toward Zn(II) at different pH values is reported in Figure 4. A 100.0 μg/2.0 mL stock solution of modified SiNPs **6** containing 1.0 μM Zn(II) solution was used for the experiment and different pH solutions were prepared as reported in the literature.[50] In acidic environments, the response is low due to protonation of the amino group in the fluorophore, which, in turn, shows low affinity toward Zn(II).[30] The fluorescence intensity, however, increases with increasing pH and a small plateau was observed between pH 7.0 to pH 8.0, and fluorescence emission intensity increases further in basic conditions up to pH 12. This increase could be attributed to deprotonation of the amino group of the fluorophore, thereby increasing its affinity toward Zn(II). The pH study shows that the use of the sensor is feasible under physiological pH (7.2−7.4).

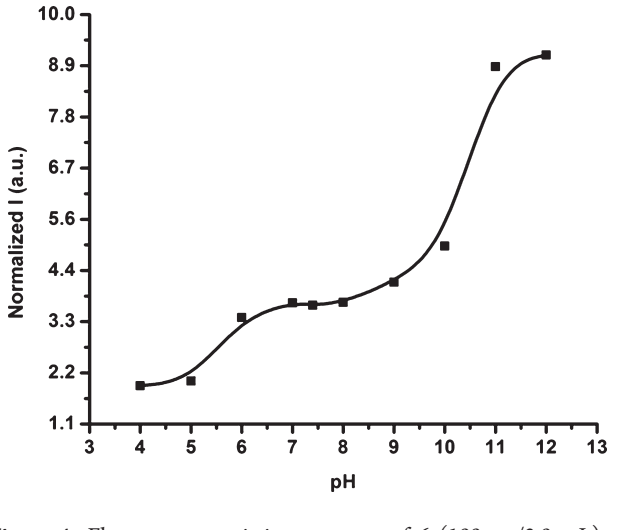

Figure 4. Fluorescence emission response of **6** (100 μg/2.0 mL) at different pH (4−12), when treated with 1.0 μM Zn(II) solution.

3.3. Zn(II) Sensing. All the metal ion detection experiments performed in this study were carried out using 100 μg of **6** in 2 mL of solvent. The amount of fluorophore on 100 μg of SiNPs was calculated by fluorescence method as described by Fang et al.[4] In this method, a calibration curve showing the relationship between the fluorescence intensity and the concentration of 8-chloroacetylaminoquinoline **4** in a solvent mixture of tris-HCl and acetonitrile (see Figure SI1 in the Supporting Information) is used to calculate the loading density of the ligand on the surface. Using the equation of a straight line (inset in Figure SI1 in the Supporting Information), and the intensity value of 4.76×10^6 corresponding to 100 μg of **6**/2.0 mL solvent gives the fluorophore concentration to be 154 ± 1.5 μM.

The detection limit of the sensor toward Zn(II) was determined by the fluorescence titration data recorded under a narrow concentration range from 0.01 to 100.0 μM (Figure 5A,B). A sharp increase in the fluorescence intensity is observed for the Zn(II) concentration of 40 μM, after which a slow increase in intensity is seen until a Zn(II) concentration of ∼80 μM, at which point a saturation effect is observed. We hypothesize a complex formation in a 1:2 mol ratio of Zn(II) to the fluorophore

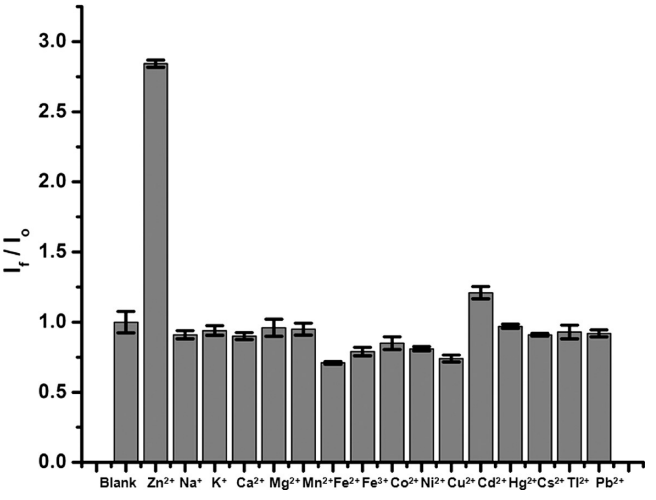

Figure 6. Bar graph of fluorescence emission intensity for sixteen different metals showing metal selectivity profile of **6** (100 μg/2.0 mL) in tris-HCl (0.01 M, pH= 7.22) with the concentration of 1.0 μM for each metal.

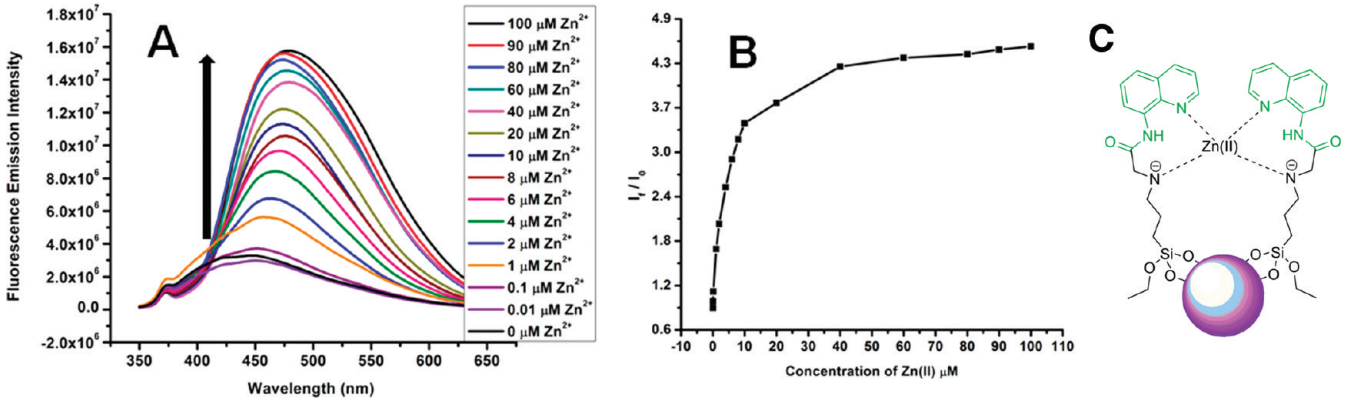

Figure 5. (A) Fluorescence emission spectra, (B) titration curve of **6** (100 μg/2.0 mL) in tris-HCl (0.01 M, pH 7.22) in the presence of Zn(II) from 0.01 to 100 μM, and (C) hypothetical figure showing capture of one Zn(II) by two fluorophores grafted on SiNPs.

dx.doi.org/10.1021/am2002394 |ACS Appl. Mater. Interfaces 2011, 3, 1731–1739

(Figure 5C). This may be explained on the basis of: 1) the ligand concentration on 100 μg SiNPs is 154 μM, which is approximately twice the amount of Zn(II), and 2) moreover, a Job's plot (see Figure SI2 in the Supporting Information), which exhibits a maximum mole fraction of Zn(II) approximately at 0.67 M,[51] further suggests the formation of a 1:2 complex. The association constant value of log K = 3.97 was obtained, which was calculated by a method developed by Descalzo et al.[52] The detection limit of the sensor was observed to be 0.1 μM of Zn(II) as shown in Figure 6A, whereas the fluorescence emission intensity increases almost 3-fold at 1 μM of Zn(II) and approximately 8-fold at 100 μM.

The UV−vis titration data of **6** with Zn(II) (0.01−100 μM concentration range) are shown in Figure SI12 in the Supporting Information. UV−vis absorption maxima increase from 0 to 4 μM concentration of Zn(II), gradually decreases from 4 to 10 μM of Zn(II), and again further increases between 10 to 100 μM of Zn(II). Absorption maxima shows a red-shift of 45 ± 5 nm (from 310 to 355 nm) in the range of 4 - 100 μM of Zn(II) concentration. There are four isosbestic points at 230, 240, 268, and 335 nm, but are not very well resolved. The UV−vis graph clearly show the change in the fluorophore absorption as concentration of Zn(II) increases in the solution.

The mechanism of fluorescence emission enhancement in both emission and absorption wavelength upon binding Zn(II) with the fluorophore is well-explained on the basis of electron transfer process.[26,34,36−39] Similar results are observed with our system, which indicates that the 8-aminoquinoline derivative **5** exhibit similar fluorescence emission and UV−vis absorption properties as compared to solution phase derivative and does not alter upon grafting on SiNPs.

The fluorescence quantum yield of **6** was calculated to be 0.043 in tris-HCl buffer (pH 7.22), which was determined by using quinine bisulphate (0.1 M H_2SO_4, Φ = 0.58) as the standard. The fluorescence emission intensity of **6** increases approximately 2.8-fold with a redshift of 55 nm upon addition of 1.0 μM Zn(II), and the quantum yield of the Zn(II) complex was calculated to be 0.1204. Within the ligand framework, the excited state proton transfer in combination with intramolecular PET causes the fluorescence to suppress, resulting in a low quantum yield.[13,26,53] Zn(II), however, can interrupt this excited state proton transfer in 8-aminoquinoline and its derivatives, and by blocking the PET process a fluorescence enhancement is observed along with an increase in the quantum yield. Zn(II), as against other late transition metals, is not capable of one-electron redox activity and, having a filled *d*-shell, cannot participate in electron transfer or energy transfer mechanisms.[36]

3.4. Metal Screening Experiments. A total of sixteen different metal ions were used for spectrofluorometric titration with the sensor **6** to establish selectivity. The metals were chosen on the basis of their biological availability, common biological elements such as sodium, potassium, calcium, magnesium, and iron, along with other late first-row transition metal ions and toxic heavy metals such as cadmium, mercury, lead, cesium, and thallium. In the first set of experiments, the fluorescence intensity was measured separately for the individual metal ions by using 1.0 μM concentration of all metal ions. The maximum fluorescence intensities are plotted in the bar graph, as shown in Figure 6. This shows the selective response for Zn(II), while the other metal ions show no or little response. The corresponding fluorescence spectrum is shown in Figure SI3 in the Supporting Information. The late transition metals from Fe to Cu exhibit slight quenching of fluorescence. These transition metals, with partially filled 3d

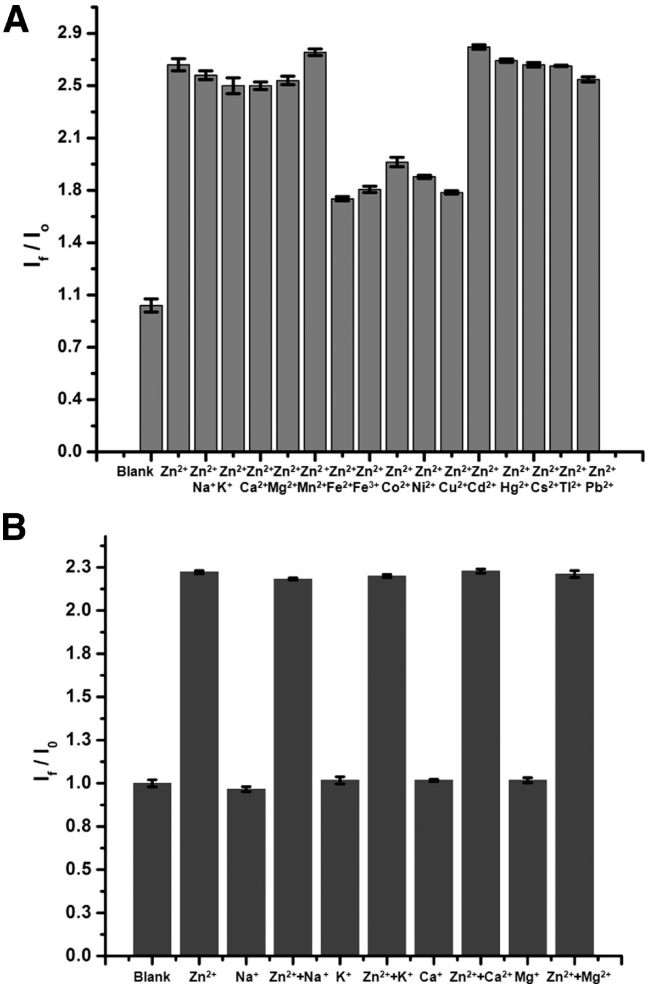

Figure 7. Relative fluorescence emission intensity of **6** (100 μg/2.0 mL) in tris-HCl (0.01 M, pH 7.22) with different metal ions in the presence of Zn(II) (A) equimolar concentrations of 1.0 μM and (B) 1.0 μM Zn(II) with other metals at 5.0 mM.

shells, exhibit redox activity, and electron exchange is possible between the fluorophore and the metal ions, resulting in the quenching of the fluorophore via nonradiative energy transfer.[1,36]

The competition of these metal ions in the presence of Zn(II) was studied in the second set of experiments. This information is essential as some of these metal ions are present at much higher concentration than Zn(II) in biological systems. Spectrofluorometric experiment with metal mixtures of Zn(II) with the other metal ions in equimolar concentrations (1.0 μM) were carried out as shown in Figure SI4A in the Supporting Information. The maximum intensities are plotted in a bar graph as shown in Figure 7A. Although, transition metals Fe through Cu compete with the binding sites, there is an overall increase in the fluorescence intensity with binding Zn(II). It should also be noted that these metal ions, with the exception of Fe(II) or Fe(III), are present in low concentration or not present in vivo.

In the third set of experiments, the concentration of the common metal ions such as Na^+, K^+, Ca^{2+}, and Mg^{2+} are at 5.0 mM, whereas maintaining the concentration of Zn(II) at 1.0 μM (Figure 7B). The higher concentration of the other metal ions does not affect the selectivity and sensitivity of the fluorophore toward Zn(II). This is clearly demonstrated from

spectrofluorometric emission spectra as shown in Figure SI4B. Each experiment for the metal ion detection was performed in triplicate, and the value reported is the average with the standard deviations ($\sigma < 2-5\%$) presented in the bar graphs.

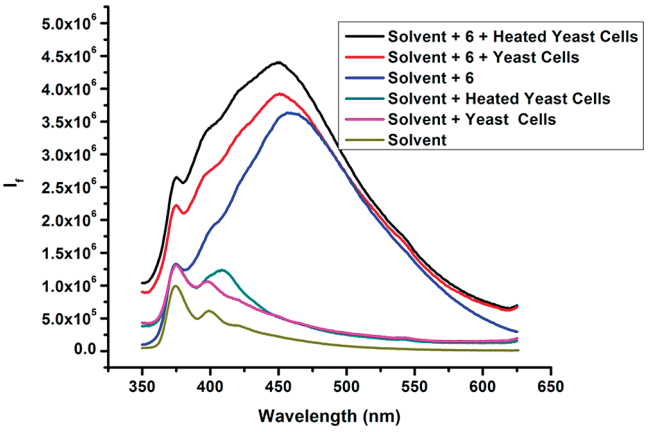

Figure 8. Fluorescence emission spectra of **6** (100 μg/2.0 mL) in tris-HCl (0.01 M, pH 7.22) after incubating with yeast cells (top two curves) and only **6** (third highest), with negative controls (lower three curves).

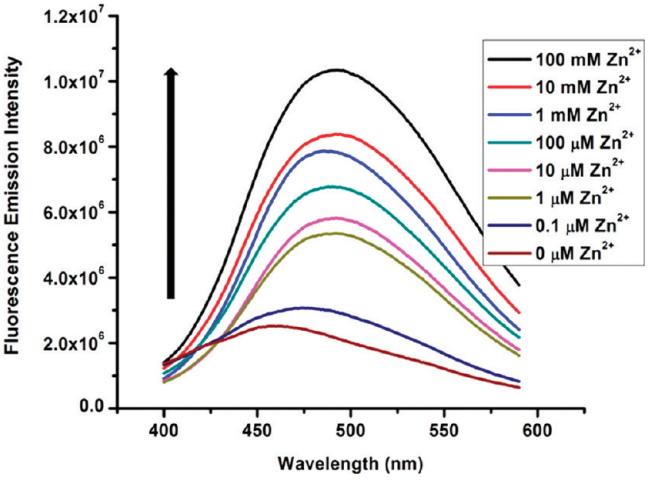

Figure 9. Fluorescence emission spectra of **6** (100 μg/2.0 mL) in the presence of Zn(II) ions from 0.1 μM to 100 mM in tap water (drinking water).

To test the application of the sensor toward Zn(II) detection in biological environment, we carried out a preliminary study with **6** in presence of yeast cells (*S. cerevisiae*). These cells are involved in the uptake and release of Zn(II) during the growth process and the use of these cells as a model for Zn(II) sensor has been previously reported.[54] Our sensor was also tested in yeast cell environment for qualitative monitoring of Zn(II). The functionalized SiNPs **6** shows enhancement of fluorescence emission in the presence of normal yeast cells and in heated cells. The control (**6**, yeast cells only, and solvent tris-HCl buffer) did not show any emission enhancement (Figure 8). The increase in the fluorescence intensities from samples suggests that shows the fluorophore could be capturing the released Zn(II) from the yeast cells. Although, using the UV−vis excitation wavelength at 330 ± 5 nm may be potentially toxic to the living cells.

Another probable application of the sensor may be for water quality monitoring of Zn(II). In order to explore this option, a second preliminary experiment was carried out in tap water. The suspension of **6** in tap water were spiked with different concentrations of Zn(II) (0.1 μM to 100 mM) and the fluorescence emission spectra were recorded as shown in Figure 9. A constant increase in fluorescence intensity was observed from lower to higher concentration of Zn(II).

The effect of different counterions on the sensor performance was also evaluated using eight different zinc salts like NO_3^-, SO_4^{2-}, CH_3COO^-, CN^-, ClO_4^{2-}, Cl^-, Br^-, and I^- at μ1 M concentration. The Figure 10A shows the fluorescence emission intensity of NPs **6** with eight different zinc salts, and the bar graph of the ratio of emission intensity is shown in Figure 10B. The maximum emission intensity was observed in case of $ZnCl_2$, which is about 7.8% is higher than the average of eight salts. Overall, the effect of different counterions on the sensor system, as compared with the nitrate counterion used for the studies, is not more than 8%.

4. CONCLUSION

A novel optical fluorometric sensor has been developed using organosilane and silica nanoparticles for sensitive and selective detection of Zn(II) in aqueous suspension. A derivative of 8-aminoquinoline was used as a metal ion chelator and fluorescent signal probe. The results of fluorescence experiments

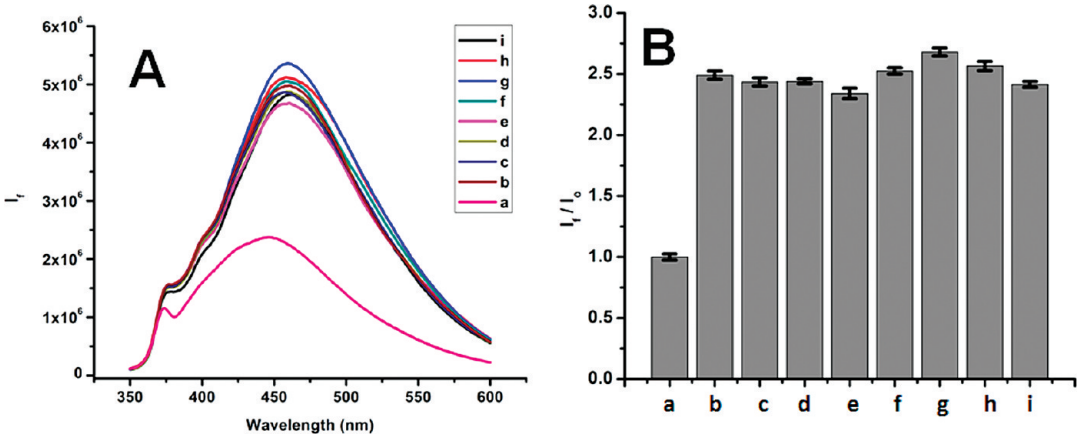

Figure 10. (A) Fluorescence emission spectra and (B) bar graph of ratio of fluorescence emission intensity, of **6** (100 μg/2.0 mL) with different zinc ions at 1 μM of concentration, where a = **6**, b = **6**+$ZnNO_3.6H_2O$, c = **6**+$ZnSO_4.7H_2O$, d = **6**+$Zn(CH_3CO)_2.2H_2O$, e = **6**+$Zn(CN)_2$, f = **6**+$Zn(ClO_4)_2.6H_2O$, g = **6**+$ZnCl_2$, h = **6**+$ZnBr_2$, and i = **6**+ZnI_2 in tris-HCl buffer.

dx.doi.org/10.1021/am2002394 |*ACS Appl. Mater. Interfaces* 2011, 3, 1731–1739

show about 2.8-fold Zn(II) enhancement in the emission intensities along with a redshift of 55 nm. The detection limit of 0.1 μM Zn(II) in tris-HCl buffer (pH 7.22) is observed. The presence of other metal ions does not affect the selectivity of the sensor, even in the presence of high concentrations (5.0 mM) of Na^+, K^+, Ca^{2+}, and Mg^{2+} along with Zn(II). Two preliminary experiments were performed to explore the applications of the sensor: (1) to detect Zn(II) in the extracellular environment, where yeast cells (*S. cerevisiae*) were used as a model and (2) to detect Zn(II) in tap water, where tap water samples were spiked with different concentrations of Zn(II). Further, eight different counterions of zinc do not affect the performance of sensor. This sensor shows selective detection of Zn(II) and can be used for Zn(II) detection in physiological environment and water quality monitoring. The performance of the sensor **6** is similar to the one we previously reported on MCM-41,[43] but higher surface loading in the former results in higher fluorescence emission intensity and quantum yield. The presence of the fluorophore on the outer surface provides better accessibility to the metal ion, which may be diffusion dependent in MCM-41, because of functionalization of the inner channels. This difference may prove to be advantageous in favor of functionalized SiNPs **6** to be used as a Zn(II) sensor.

■ ASSOCIATED CONTENT

Supporting Information. Experimental procedures for synthesis of **2** to **6**, ^{1}H, ^{13}C, ^{29}Si NMR of **5**; solid-state ^{13}C, ^{29}Si NMR **6**; fluorescence emission intensity of calibration curve of **5**, fluorescence emission spectrum of **6** with 15 metal ions, job's plot of **6**, fluorescence emission spectrum of **6** with 15 metal ions + Zn(II), fluorescence emission spectrum of **6** in the presence of high concentration of metal ions, UV−vis absorption spectra of **2** to **6**, fluorescence excitation spectra of **6**, and UV−vis absorption titration analysis of 6 with Zn(II) (PDF). This material is available free of charge via the Internet at http://pubs.acs.org/.

■ AUTHOR INFORMATION

Corresponding Author

*Phone: +1-208-885-7277. Fax: +1-208-885-6173. E-mail: srastogi@uidaho.edu.

Author Contributions

‡The first two authors have contributed equally toward this manuscript.

■ ACKNOWLEDGMENT

The financial support from the U.S. Department of Agriculture (2009-34479-19833, and 2010-34479-20715) and the Center for Biological Applications of Nanotechnology (BANTech) group at the University of Idaho (UI) are gratefully acknowledged. The authors would like to thank Franklin Bailey (electron microscopy center facility at the UI) for providing TEM images of SiNPs, Jeanne Shreeve, Department of Chemistry at the UI, for providing elemental analyzer and TGA facility, and Alexander Blumenfeld, Department of Chemistry at the UI for NMR.

■ REFERENCES

(1) Valeur, B.; Leray, I. *Coord. Chem. Rev.* **2000**, *205*, 3–40.
(2) Chow, C. F.; Lam, M. H. W.; Leung, M. K. P. *Anal. Chim. Acta* **2002**, *466*, 17–30.
(3) Zhaochao, X.; Yi, X.; Xuhong, Q.; Jingnan, C.; Dawei, C. *Org. Lett.* **2005**, *7*, 889–892.
(4) Lu, F. T.; Gao, L. N.; Li, H. H.; Ding, L. P.; Fang, Y. *Appl. Surf. Sci.* **2007**, *253*, 4123–4131.
(5) Li, H.; Zhang, Y.; Wang, X.; Gao, Z. *Microchim Acta.* **2008**, *160*, 119–123.
(6) Leng, B.; Zou, L.; Jiang, J.; Tian, H. *Sens. Actuatores, B* **2009**, *140*, 162–169.
(7) Zhen, J.; Xiao-Bing, Z.; De-Xun, X.; Yi-Jun, G.; Jing, Z.; Xin, C.; Guo-Li, S.; Ru-Qin *Anal. Chem.* **2010**, *82*, 6343–6346.
(8) Kumar, M.; Kumar, R.; Bhalla, V. *Org. Lett.* **2011**, *13*, 366–369.
(9) Panday, P. C.; Prakash, R. *Sens. Actuators, B* **1998**, *46*, 61–65.
(10) Nguyen, T.; Rosenzweig, Z. *Anal. Bioanal. Chem.* **2002**, *374*, 69–74.
(11) Gupta, V. K.; Jain, A. K.; Maheshwari, G. *Talanta* **2007**, *72*, 49–53.
(12) Sumner, J. P.; Kopelman, R. *Analyst* **2005**, *130*, 528–533.
(13) Mu, L.; Shi, W.; Chang, J. C.; Lee, S. T. *Nano Lett.* **2008**, *8*, 104–109.
(14) Fan, J.; Peng, X.; Wu, Y.; Lu, E.; How, J.; Zhang, R. Z.; Fu, X. *J. Lumi.* **2005**, *114*, 125–130.
(15) Silvia, J.; Williams, R. Claridon Press: Oxford, 1991.
(16) Ruedas-Rama, M. J.; Hall, E. A. H. *Anal. Chem.* **2008**, *80*, 8260–8268.
(17) Berg, J. M.; Shi, Y. *Science* **1996**, *271*, 1081–1085.
(18) Vallee, B. L.; Falchuk, K. H. *Physiol. Rev.* **1993**, *73*, 79–118.
(19) Suh, S. W.; Jensen, K. B.; Jensen, M. S.; Silva, D. S.; Kesslak, P. J.; Danscher, G.; Fredrickson, C. 2000, *852*, 274-278.
(20) Choi, D. W.; Koh, J. Y. *Annu. Rev. Neurosci.* **1998**, *21*, 347–375.
(21) Weiss, J. H.; Sensi, S. L.; Koh, J. Y. *Trends Pharmacol. Sci.* **2000**, *21*, 395–401.
(22) Saha, U. C.; Chattopadhyay, B.; Dhara, K.; Mandal, S. K.; Sarkar, S.; Khuda-Bukhsh, A. R.; Mukherjee, M.; Helliwell, M.; Chattopadhyay, P. *Inorg. Chem.* **2011**, *50*, 1213–1219.
(23) Li, J.; Meng, J.; Huang, X.; Cheng, Y.; Zhu, C. *Polymer* **2010**, *51*, 3425–3430.
(24) Jin, Z.; Zhang, X. B.; Xie, D. X.; Gong, Y. J.; Zhang, J.; Chen, X.; Shen, G. L.; Yu, R. Q. *Anal. Chem.* **2010**, *82*, 6343–6346.
(25) Sarkar, K.; D, K.; N, M.; Roy, P.; Bhaumik, A.; Banerjee., P. *Adv. Funct. Mater.* **2009**, *19*, 223–234.
(26) Jiang, P.; Guo, Z. *Coord. Chem. Rev.* **2004**, *248*, 205–229.
(27) Teolato, P.; Rampazzo, E.; Arduini, M.; Mancin, F.; Tecilla, P.; Tonellato, U. *Chem.—Eur. J.* **2007**, *13*, 2238–2245.
(28) Frederickson, C. J.; Kasarkis, E. J.; Ringo, D.; Frederickson, R. D. *J. Neurosci. Meth.* **1987**, *20*, 91–103.
(29) Zalewski, P. D.; Forbes, I. J.; Betts, W. H. *Biochem. J.* **1993**, *296*, 403–408.
(30) Zalewski, P. D.; Forbes, I. J.; Seamark, R. F.; Borlinghaus, R.; Bette, W. H.; Lincoln, S. F.; Ward, A. D.; Zinquin *Chem. Biol.* **1994**, *3*, 153–161.
(31) Mahadevan, I. B.; Kimber, M. C.; Lincoln, S. F.; Tiekink, E. R. T.; Ward, A. D.; Betts, W. H.; Forbes, I. J.; Zalewski, P. D. *Aust. J. Chem.* **1996**, *49*, 561–568.
(32) Budde, T.; Minta, A.; White, J. A.; Kay, A. R. *Neuroscience* **1997**, *79*, 347–358.
(33) Chen, Y.; Han, K.-Y.; Liu, Y. *Bioorg. Med. Chem.* **2007**, *15*, 4537–4542.
(34) Zhang, Y.; Guo, X.; Si, W.; Jia, L.; Qian, X. *Org. Lett.* **2008**, *10*, 473–476.
(35) Dong, Z.; Yang, B.; Jin, J.; Li, J.; Kang, H.; Zhong, X.; Li, Rong; Ma, J. *Nanoscale Res. Lett.* **2009**, *4*, 335–340.
(36) Fabbrizzi, L.; Licchelli, M.; Pallavicini, P.; Sacchi., D.; Taglietti *Analyst* **1996**, *121*, 1763.
(37) Williams, J. N.; Reibenspies, J. H.; Hancock, R. D. *Inorg. Chem.* **2009**, *48*, 1407–1415.
(38) Burdette, S. C.; Frederickson, C. J.; Bu, W.; Lippard, S. J. *J. Am. Chem. Soc.* **2003**, *125*, 1778–1787.
(39) Huston, M. H.; Haider, K. W.; Czarnik, A. W. *J. Am. Chem. Soc.* **1988**, *111*, 4460–4462.

(40) Balzani, V.; Bolletta, F.; Gandolfi, M. T.; Maestri, M. *Top. Curr. Chem.* **1978**, *75*, 1–64.
(41) de Silva, A. P.; Gunaratne, H. Q. N.; Gunnlaugsson, T.; Huxley, A. J. H.; McCoy, C. P.; Rademacher, J. T.; Rice, T. E. *Chem. Rev.* **1997**, *97*, 1515–1566.
(42) de Silva, A. P.; Fox, D. B.; Huxley, A. J. H.; Moody, T. S. *Coord. Chem. Rev.* **2000**, *205*, 41–57.
(43) Callan, J. F.; de Silva, A. P.; Magri, D. C. *Tetrahedron* **2005**, *61*, 8551–8588.
(44) Pal, P.; Rastogi, S. K.; Gibson, C. M.; Aston, D. E.; Branen, A. L.; Bitterwolf, T. E. *ACS Appl. Mater. & Inter.* **2010**, *3*, 279–286.
(45) Zou, H.; Wu, S.; Shen, P. J. *Chem. Rev.* **2008**, *108*, 3893–3957.
(46) Jaroniec, C. P.; Gilpin, R. K.; Jaroniec, M. J. *J. Phys. Chem. B* **1997**, *101*, 6861–6866.
(47) Iler, R. K. Wiley: New York, 1979.
(48) Jaroniec, C. P.; Kruk, M.; Jaroniec, M.; Sayari, A. *J. Phys. Chem. B* **1998**, *102*, 5503–5510.
(49) Yokoi, T.; Tatsumi, T.; Yoshitake, H. *J. Colloid Interface Sci.* **2004**, *274*, 451–457.
(50) David, D. Moore, *Current Protocols in Molecular Biology*;John Wiley and Son: New York, 1996; appendix A.2.1−A.2.8.
(51) Zachary, D. H.; Patrick, M. C. *J. Chem. Educ.* **1986**, *68*, 162–167.
(52) Descalzo, A. B.; Marcos, M. D.; Martínez-Máñez, R; Soto, J; Beltrán, D.; Amorós, P. J. *Mater. Chem.* **2005**, *15*, 2721–2731.
(53) van Meervelt, L.; Goethals, M.; Leroux, N.; Zeegers-Huyskens *J. Phys. Org. Chem.* **1997**, *10*, 680–686.
(54) Simm, C.; Lahner, B.; Salt, D.; LeFurgey, A.; Ingram, P.; Yandell, B.; Eide, D. J. *Biochem. Biophys. Res. Commun.* **2004**, *323*, 58–64.